

TRMM RAINFALL PRODUCTS AND TOOLS FOR TROPICAL INFECTIOUS DISEASE STUDIES

Zhong Liu*¹, L. Chiu¹, W. Teng², H. Rui², and G. Serafino
 GSFC Earth Sciences Data and Information Services Center
 Distributed Active Archive Center (DAAC)
 NASA/Goddard Space Flight Center, Greenbelt Maryland, USA 20771
¹CEOSR, George Mason University, Fairfax, VA
²SSAI, Lanham, MD

1. INTRODUCTION

Recent studies have revealed that many tropical infectious diseases are linked to weather and climate. In several case studies, investigators have found that above normal warm temperatures and rainfall during El Nino events were linked to outbreaks of many tropical diseases, such as, leptospirosis, bartonellosis, Rift Valley fever, hantavirus pulmonary syndrome, malaria, Ross River virus, etc. (e.g., Anyamba et al., 2000; Zhou et al., 2002; Masuoka et al., 1998). Along with other environmental parameters, rainfall has also been used in many disease related applications, such as, mapping malaria distribution in West Africa. However, in many tropical regions, rainfall estimates still remain a major challenge due to sparse rain gauges. To better understand tropical disease transmission and develop applications for these regions, it is necessary to have rainfall data with adequate spatial and temporal resolutions.

2. DATA PRODUCTS AND TOOLS

The Tropical Rainfall Measuring Mission (TRMM) is a joint U.S.-Japan satellite mission to monitor tropical and subtropical (40°S - 40°N) precipitation and to estimate its associated latent heating. The TRMM provides the first detailed and comprehensive dataset on the four dimensional distribution of rainfall and latent heating over vastly undersampled tropical and subtropical oceans and continents. The TRMM satellite was launched on November 27, 1997. Data from the TRMM are archived and distributed by the GSFC Earth Sciences Data and Information Services Center (GDISC). In August 2001, the TRMM was boosted from an altitude of 350 km to 402.5 km, thus extending the satellite life span and data collection for few more years.

The TRMM satellite flies at an altitude of 350 km with a period of 91.5 minutes. The TRMM satellite carries three rain-measuring instruments. NASA GSFC provided the TRMM Microwave Imager (TMI), the Visible Infrared Scanner (VIRS), and the observatory, and operates the TRMM satellite via the Tracking and Data Relay Satellite System (TDRSS). The National Space Development Agency (NASDA) of Japan provided the Precipitation Radar (PR), the first space-borne

precipitation radar, and launched the TRMM observatory. Table 1 summarizes the TRMM standard products available at the Goddard DAAC. Level 1 products are the VIRS calibrated radiances, the TMI brightness temperatures, and the PR return power and reflectivity measurements. Level 2 products are derived geophysical parameters at the same resolution and location as those of the Level 1 source data. Level 3 products are the time-averaged parameters mapped onto a uniform space-time grid. An evaluation of the sensor, algorithm performance and first major TRMM results appear in the Special Issue on the Tropical Rainfall Measuring Mission (TRMM), the combined publication of the Journal of Climate and Journal of Applied Meteorology (2000).

	Visible Infrared Scanner	TRMM Microwave Imager	Precipitation Radar	Combined Products	Ground Validation (GV)
Level 1	Visible & IR radiances	Microwave brightness temperatures	Radar return power & reflectivity	NA	Cal radar reflectivity at each GV site
Level 2	NA	TMI profile for CLW, prec. water, cloud ice, prec. ice, latent heat, & surface rain	PR surface cross-section & path attenuation, rain type, storm, & freezing height, PR profile for rain rate, reflect., attenuation, & rain top/bottom height	Rain rate, drop size dist. parameters, path integrated attenuation	Rain existence, rain map, rain type, 3-D reflectivity, rain gauge, disdrometer
Level 3	NA	TMI monthly rainfall, rain rate, rain frequency, & freezing height	PR monthly surface rain total, rain profile at 2, 4, 6, 10 & 15 km, fractional rain, storm height histogram, snow ice layer, surface rain rate, & path attenuation	Monthly surface rainfall, CLW, rain water, cloud ice, & graupel; combined instruments calibration, global gridded rainfall	Rain map, 3-D map

Table 1. TRMM standard products at Goddard DAAC .

* Corresponding author address: Zhong Liu, GMU/DAAC, NASA/GSFC, Code 902, Greenbelt, MD 20771; Email: zliu@daac.gsfc.nasa.gov

Many previous disease studies show that precipitation is not the only climate parameter related to diseases outbreaks. To obtain a complete picture of local and regional environmental conditions, it is necessary to include other climate data sets for analyses. Willmott and Matsuura (1995) applied various techniques to estimate global climate variables based on surface observations between 1950 – 1999. Data sets from satellites, such as, NOAA Pathfinder Normal Difference Vegetation Index (NDVI), are also included.

Currently, it is not easy for health investigators to obtain local and regional environmental conditions. They often have to deal with data sets in different formats. To conduct data processing, one often has to learn or write the processing software, which can sometimes be very time consuming and thus limit the number of environmental data sets one can examine.

To overcome these obstacles, the Hydrology Data Support Team (HDST) at the DAAC has begun to develop tools for analyzing and visualizing global gridded environmental data sets. Simple statistics such as area averages and time series over specific areas can be computed and displayed on-line. The following case studies will show how these tools are used in tropical infectious disease studies.

3. CASE STUDIES

a. Bartonellosis epidemics in Peru

Bartonellosis epidemics in Peru (Figure 1) have been reported and studied by a number of investigators (e.g., Zhou et al., 2002; Masuoka et al., 1998). Bartonellosis is a bacterial disease endemic and it is believed that the bacterium, *Bartonella bacilliformis* (Bb), is transmitted to humans by the bite of the sand fly. Masuoka et al. (2002) revealed that the typical breeding places are under stones, in masonry cracks, in poultry houses or other areas combining darkness, humidity and a supply of organic material for food. Incidence of the disease usually begins to rise in December, peaks in February and March, and decreases to the lowest between July and November (Zhou et al. 2002). The study (Zhou et al., 2002) showed that the bartonellosis epidemics were more sensitive to the local temperature increases than to the rainfall anomaly.

With the DAAC's online analysis tools, one can quickly assess the environmental conditions in the region and find out anomalies that are related to climate changes. We will use the bartonellosis epidemics in Peru in 1998 as an example to demonstrate the use of these tools. In order to assess the regional environmental conditions, a region [20°S – EQ; 67°W – 82°W] has been selected. Figure 2 shows the time series of the regional average air temperature during 1950 – 1999. It shows that the monthly air temperature in January, 1998 is the highest. The time series also shows a gradual warming trend in the region.



Source: <http://www.odci.gov/cia/publications/factbook/index.html>

Figure 1. A map of Peru.

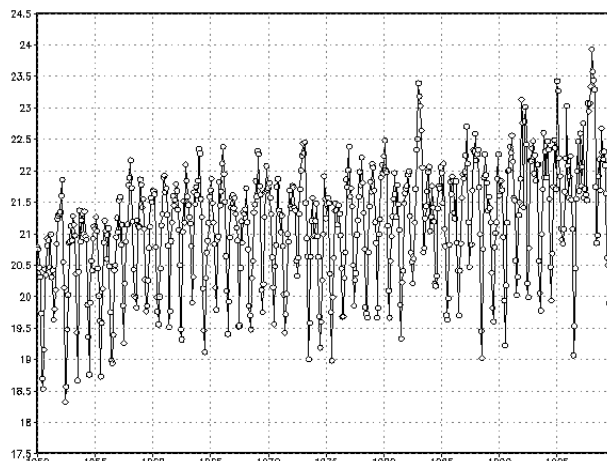


Figure 2. Time series of the regional average air temperature in degree Celsius .

The regional average rainfall (Figure 3) shows that no significant change in the monthly rainfall in the early 1998. The average rainfall from Willmott and Matsuura (1995) (not shown) has also confirmed this. Figures 4 and 5 are the similar time series except for snow melt and evapotranspiration, respectively. The high snow melt and the recording breaking evapotranspiration are also found in the time series. Figure 6 is the time series of the regional average NDVI. It shows that the NDVI in May 1998 is the second highest in the records. Figure 7 is the regional plot for that month. Due to the limited space, only these variables are plotted. Users can plot the others by visiting the link listed at the end of this article.

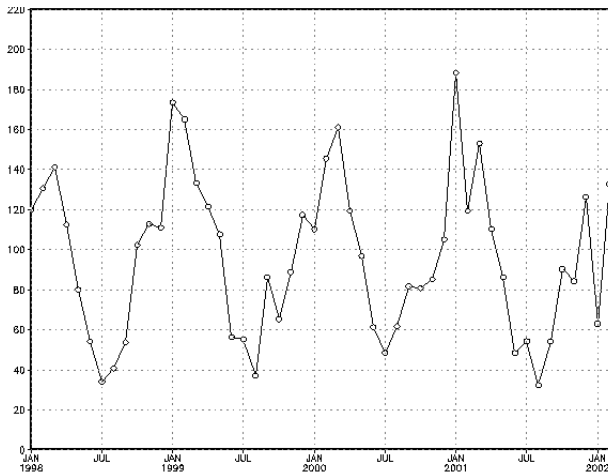


Figure 3. Time series of the regional average TRMM 3B43 monthly rainfall (in mm).

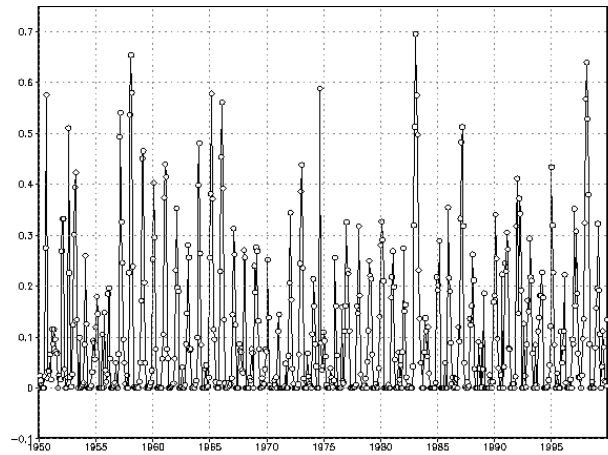


Figure 4. Time series of the regional average snow melt (in mm).

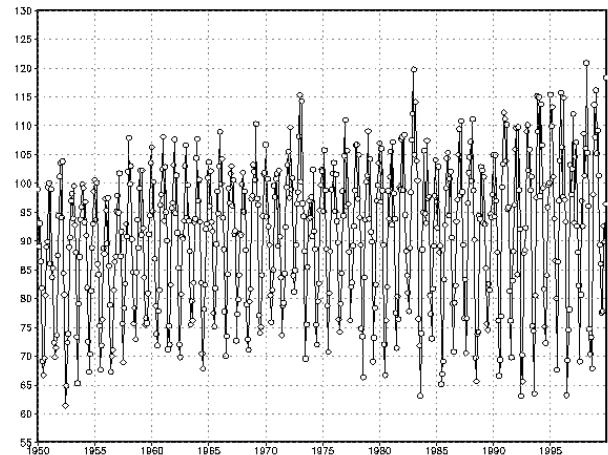


Figure 5. Time series of the regional average actual evapotranspiration (in mm).

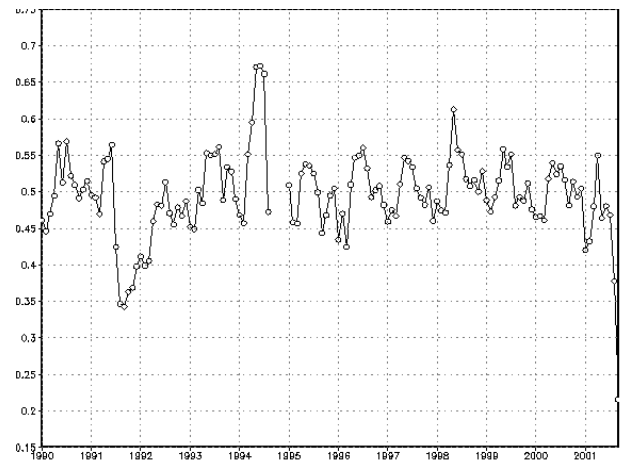


Figure 6. Time series of the regional average NDVI.

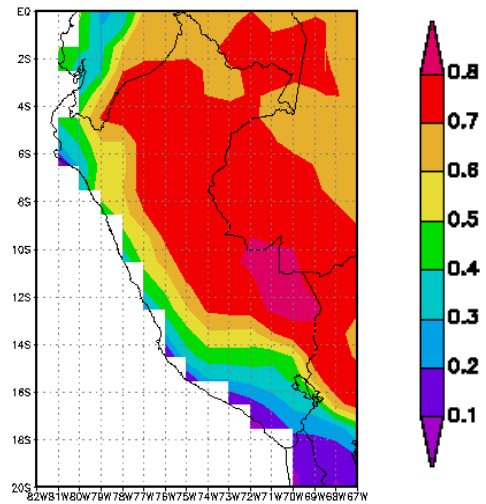


Figure 7. Regional map of NDVI for May 1998.

In conclusion, the record breaking air temperatures, which occurred prior to other record breaking events in the region, have been identified via the analysis. Due to the lack of understanding of the habitat and behavior of the sand flies at the time being, additional studies are needed to link these climate anomalies to the increasing population of the sand flies reported in the region.

b. Rift Valley Fever epidemics in East Africa

Rift Valley Fever epidemics in East Africa (Figure 8) have been studied by a number of investigators (e.g., Anyamba et al. 2000; 2001; 2002). The studies showed that the time series of NDVI can be used for predictions of the epidemics. We select the reported outbreaks during the 1997/98 months. Like the previous case study, we select a box [2°S – 6°N; 32°E – 42°E] to represent the Rift Valley region. With the DAAC's tools, one can quickly examine the environmental conditions.



Figure 8. A map of Kenya.

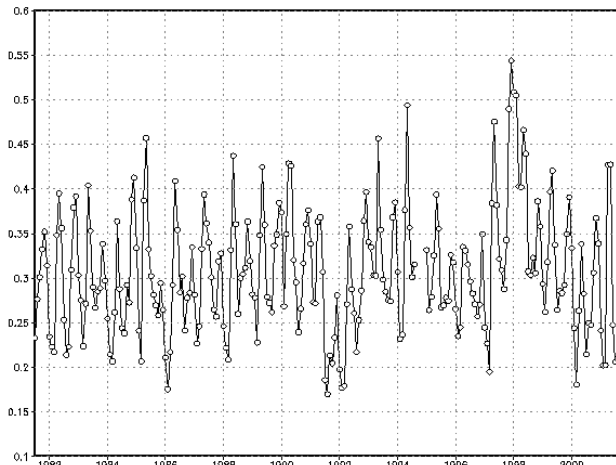


Figure 9. Time series of the regional average NDVI.

The time series of NDVI (Figure 9) shows that the record breaking NDVI is found in December of 1997. The regional NDVI map (Figure 10) gives a detailed spatial distribution. Examining the rainfall for the region (Figure 11), it shows the near recording breaking rainfall is found in November of 1997. It appears that the high NDVI was the result of the high rainfall in the previous month. Figure 12 is the time series of the regional average air temperature. It is found that the monthly average air temperatures during the months of 1997 and 1998 are not significantly higher or lower than the other years. As mentioned earlier, TRMM provides more rainfall information than the sparse rain gauges in tropics. Figure 13 is a four-year average rainfall map. It

shows the rainfall patterns over Lake Rudolf, Lake Victoria and the Indian Ocean.

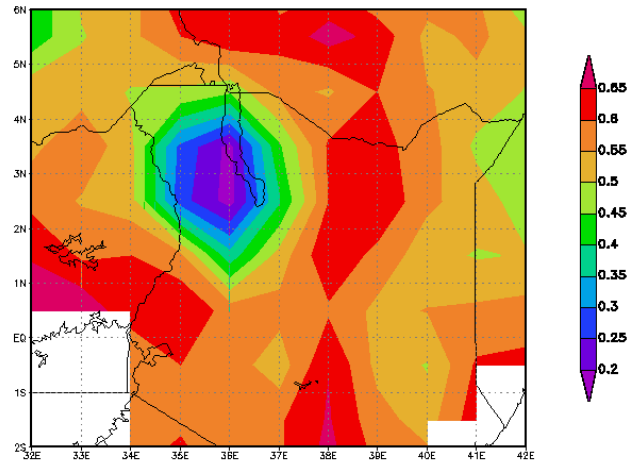


Figure 10. Regional map of NDVI for December, 1997.

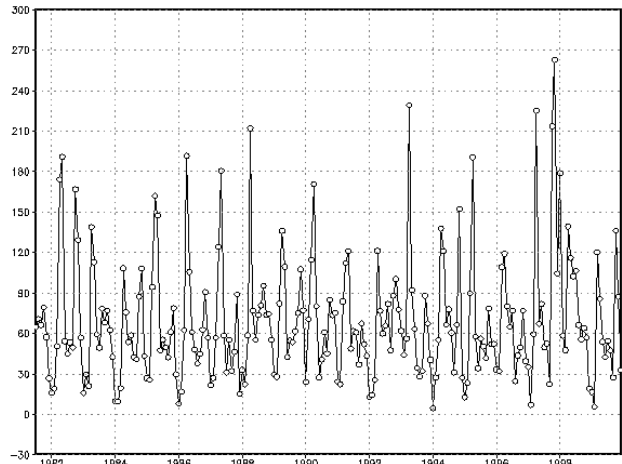


Figure 11 Time series of the regional average rainfall (in mm).

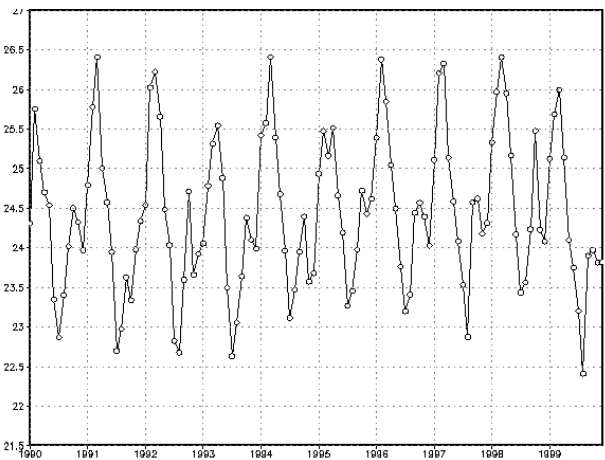


Figure 12 Time series of the regional average air temperature (in degree Celsius).

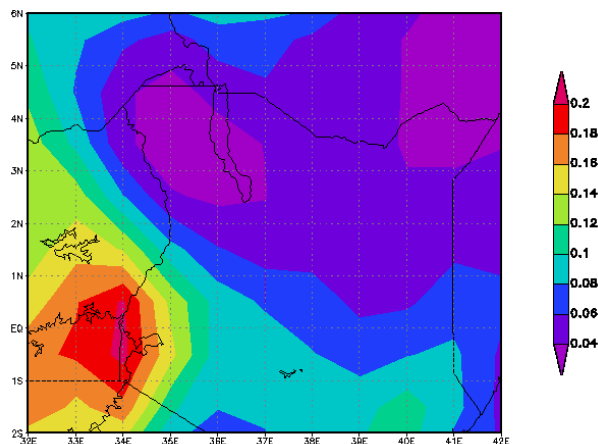


Figure 13. Regional map of the four-year (1998-2001) average rain rate (in mm/hour) computed from the TRMM 3B43 monthly product.

4. CONCLUSIONS AND FUTURE PLANS

With examples, this poster has demonstrated the use of TRMM, other climate data, and the tools for tropical infectious disease studies. The poster also has demonstrated the use of the easy and simple tools developed by the DAAC for assessing local and regional environment conditions. In the future plans, more data sets, including model prediction data and data sets in high spatial and temporal resolutions, will be added in order to obtain a more complete picture of past and future local and regional climate and environmental conditions. More functions and features that are user friendly will be added as well.

The two case studies have shown a strong link between the climate changes and the disease outbreaks, though more detailed studies are still needed in order to understand the responses of different vectors to climate changes. The case studies have also shown that the regional climate systems were very complicated, for example, in both cases, according to the previous studies (Zhou et al., 2000; Anyamba et al., 2000), the El Nino event had a strong influence on the climate systems in both regions, but, as we have seen from the case studies, the responses were very different. In Peru, the record breaking air temperatures occurred and in Kenya, the near record high rainfall. The high NDVI values were found in both regions, but they are explained differently. In Peru, the abnormally high NDVI was not directly linked to the normal rainfall and the melting snow was too small to make a significant contribution. It is not certain whether the record breaking evapotranspiration (which was nearly equal to the monthly rainfall) was the main contributor and further studies are needed. In Kenya, it appears that the heavy rainfall that occurred prior to the event was the main contributing factor to the high NDVI.

REFERENCES:

Anyamba, A., K.J. Linthicum, and R.L. Mahoney, 2000: Application of NDVI Time Series Data to Monitor Rift Valley Fever Outbreak Patterns. Proceedings of The Twenty-Fifth Annual Climate Diagnostics and Prediction Workshop, Palisades, New York.

Masuoka, P., J. Gonzalez, S. Gordon, N. Achee, P. Pachas, R. Andre, and L. Laughlin, 2002: Remote Sensing and GIS Studies of Bartonellosis in Peru", Poster Presentation at High Spatial Resolution Commercial Imagery Workshop, Reston, VA.

Special Issue on the Tropical Rainfall Measuring Mission (TRMM), combined publication of the December 2000 *Journal of Climate* and Part 1 of the December 2000 *Journal of Applied Meteorology*, American Meteorological Society, Boston, MA.

Willmott, C. J. and K. Matsuura, 1995: Smart Interpolation of Annually Averaged Air Temperature in the United States. *Journal of Applied Meteorology*, 34, 2577-2586.

Zhou, J., Lau, W.K., P. Masuoka, R.G. Andre, J. Chamberlin, P. Lawyer, L.W. Laughlin, 2002. El Nino and the Spread of Bartonellosis Epidemics in Peru. *EOS, Transactions - American Geophysical Union* 83(14), 157-161.

INFORMATION:

Online analysis tools for TRMM rainfall products, NDVI, TOMS aerosols and Willmott climate data:

http://esip.gmu.edu/esip/ES_gridded_online_analysis_gmu.html

Data in higher temporal and spatial resolutions:

<http://eosdata.gsfc.nasa.gov/data/>

All TRMM standard data can be searched and ordered via:

<http://lake.nascom.nasa.gov/data/dataset/TRMM>

For further details about TRMM, visit:

<http://trmm.gsfc.nasa.gov>

Questions and comments, please email to:

hydrology@daac.gsfc.nasa.gov